Journal of Chromatography, 186 (1979) 317–338

CHROM. 12,192

COMPREHENSIVE STUDY OF POROUS POLYMERIC STATIONARY PHASES FOR CHROMATOGRAPHY

DENG LI-RU
Institute of Chemistry, Academia Sinica, Peking (People's Republic of China)

SUMMARY

A comprehensive study of spherical polymeric beads for use as chromatographic packings is presented. These include porous polydivinylbenzene, porous carbon beads prepared from poly(vinylidene chloride) and cross-linked polystyrene ion-exchange resins. The synthetic methods and the applications of these beads and the relationships between physico-chemical properties and chromatographic performance were investigated.

INTRODUCTION

Synthetic polymers have been increasingly used as column packings since Hollis[1] developed the Porapak series. In 1969, we began to study the relationships between chromatographic performance and the functional groups in and skeletal structure of the macromolecules, and also the pore structure and surface properties of polymeric micro-beads. Three series of polymer-based stationary phases for gas chromatography (GC) and liquid chromatography (LC) have been developed: GDX, TDX and YSG. They are all now being produced commercially and used extensively. This paper deals mainly with a study of the synthesis of the packings, their fundamental properties and applications and a preliminary study of the mechanism of chromatographic separation.

GDX COPOLYMER BEADS FOR GC

GDXs are divinylbenzene–ethylstyrene copolymers with or without a polar monomer, synthesized in the presence of a diluent. These highly porous polymers with strong hydrophobic macromolecular chains give sharp and symmetrical water peaks. They are best suited for some specific analyses that are difficult to achieve with conventional column packings, *e.g.*, the chromatographic determination of trace amounts of water in polar organic and inorganic compounds. In addition to their outstanding selectivity, they are thermally stable, give negligible bleeding, and hence are suitable for use in both process and preparative chromatographs.

Both applications and elucidations of the separation mechanism have been

attempted by modifying the chemical compositions and pore structures of the copolymers.

Some essential factors in the synthesis of porous copolymer beads

Influence of functional groups and skeletal structure on selectivity. The general requirements for a column packing are a rigid skeleton, high permeability and thermal stability and insensitivity to the mobile phase. As ethylstyrene–divinylbenzene beads are copolymerized in the presence of a diluent, the hydrophobic macromolecules will propagate in different manners in different kinds and amounts of solvents. Thus, a series of non-polar stationary phases can be formed with various porosities and specific surface areas.

According to the physico-chemical properties of the substances to be separated, suitable polar monomers are selected for copolymerization with divinylbenzene in order to facilitate interactions between the components to be separated and the functional groups in the polymer. Different types of GDX have different selectivities[2]. The retention indices of water increase progressively when the polarity of the comonomer is increased from GDX-1 to -5, as shown in Table I. In most instances water elutes with a symmetrical peak before propane or butane, except on GDX-5. Hence the retention time of water can be adjusted so as to offer good separation and accurate quantitation.

TABLE I

RETENTION INDICES OF WATER ON GDX COLUMNS

GDX-102	*GDX-203*	*GDX-303*	*GDX-401*	*GDX-501*
247.6	254.3	304.2	331.6	556.0

The selectivity of the polar polymer depends greatly on the kind and amount of the polar monomer used. It is evident that pyrrolidone groups in the macromolecular network play the main role in separating water well from hydrogen chloride. The relative retention (α) in GDX-401 is 5.5, which is about one order of magnitude higher than that in non-polar packings. It was considered that the elution of hydrogen chloride molecules was retarded owing to hydrogen bond formation with the nitrogen atoms of the pyrrolidone groups. Another example is the separation of benzene from cyclohexane on a highly polar stationary phase having nitro groups. Fig. 1 is a plot of the specific retention volume *versus* the reciprocal of absolute temperature. The changes in the enthalpy of cyclohexane and benzene calculated from the slopes are 14.2 and 15.3 kcal/mol, respectively. This indicates that the interaction force is larger for benzene because of its π-electron. C_4 alkane and olefin isomers are difficult to separate because of their close boiling points. However, their dipole moments and polarizabilities are different. When we selected a suitable polar monomer copolymerized with divinylbenzene, a good separation resulted at optimal polar monomer content (M). If M is fixed, the relative retentions of each component are nearly constant, despite the variation of the diluent content. This further confirms that functional groups play the major role in the separation process.

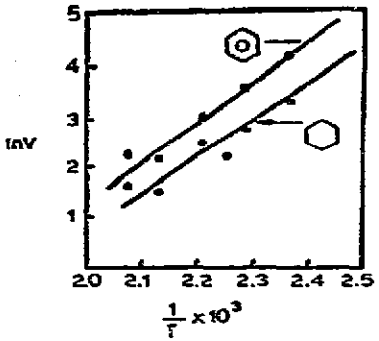

Fig. 1. Temperature dependence of retention of benzene and cyclohexane on GDX-601.

Influence of pore structure on chromatographic performance. It is very important to make the porosity of the polymer beads optimal so as to facilitate mass transfer. Moore[3] proposed that if an inert solvent were added to the monomer, the polymer synthesized would possess a real pore structure. The porosity could then be controlled by selecting the cross-linking agent on the one hand and by using different kinds and amounts of solvent on the other. During polymerization microgels are formed first, which then swell and propagate further. Finally, a cross-linked skeleton is obtained with relative fixed positions, and real pores exist after the diluent has been removed. Under ordinary conditions, the use of a poor solvent as the diluent resulted in large real pores, because the coherence of the microgels is larger than the interaction between the microgels and the solvent. The reverse will be the case if a good solvent is used (*e.g.*, in GDX-105). Table II gives data on the pore structures of some non-polar GDXs. As the amount of the diluent increases, the apparent density decreases with increase in the real pore diameter, and the specific surface area increases. A tentative explanation will be given here to account for the high efficiency of GDX-203 in which 80% of diluent was used.

TABLE II

DEPENDENCE OF PORE SIZE ON AMOUNT OF DILUENT

Diluent (%)	*Apparent density (g/ml)*	*Specific surface area (m^2/g)*	*Pore size**
50	0.28	330	
60	0.20	680	
80	0.09	800	
			↓ Increase

* Pore size estimated from electron microscopy.

The thickness of the network membranes inside the beads calculated from the specific surface area and skeleton density is approximately 10–10^2 Å, hence rapid mass transfer would be expected. This is why GDX-203 is the best choice for resolving high-boiling compounds such as C_{10}–C_{20} alkanes, while for rare gases GDX-105 is preferred.

Evidently, porosity is an important factor in addition to chemical composition. Fig. 2 shows the optimal specific surface area (and hence porosity) in relation to column efficiency.

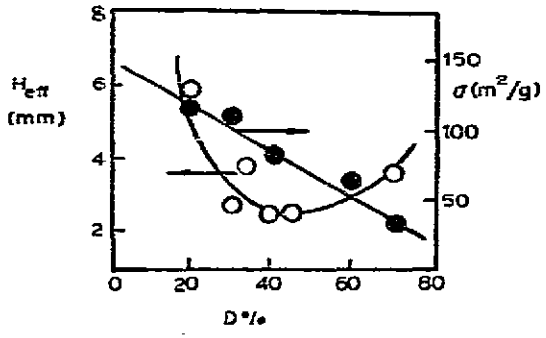

Fig. 2. Content of diluent *versus* column efficiency and specific surface area with fixed chemical composition of the polymer. $T_c = 108°$. Column: 2 m × 3 mm I.D. Sample: 1,3-butadiene.

The interaction between macromolecular chains and diluent molecules during polymerization became especially noticeable at high concentrations of polar monomer. In such a case, an optimal amount of polar solvent is added in order to maintain a reasonable interaction between those molecules, otherwise the real pores of the polymer would be distributed inhomogeneously and the beads obtained would be like hollow spheres, fragile and unusable.

Influence of shape of particles on chromatographic behaviour. Beads of spherical shape are more desirable for achieving a high performance than are irregular beads by reducing the eddy diffusion term in the Van Deemter equation ($H = A + B/u + Cu$). Incidently, spherical beads can easily be produced by suspension polymerization. The use of very finely powdered calcium carbonate, poly(vinyl alcohol) and a compound dispersant (epoxychloropropane–tetraethylenepentaamine and Bentonite) has been studied in our laboratory. Of these, the compound dispersant is particularly effective for sphere formation and suitable for the synthesis of highly polar polymers.

Gas chromatographic characteristics of GDX

An approach to the evaluation of GDXs is to measure the Kováts retention indices (I) of various kinds of organic compounds on them. An advantage of the retention index system is the almost linear dependence of I on temperature. From the results obtained[4], it was found that GDXs were superior for the analysis of permanent and rare gases or C_1–C_3 hydrocarbon mixtures at room temperature. The selectivity toward many kinds of organic compounds such as alcohols, ketones, acids, esters, ethers, aldehydes, nitrogen-containing compounds, halogenated alkanes, aromatics and their homologues were studied. Sharp and symmetrical peaks were obtained if the column temperature was slightly higher than the boiling point of the solutes.

As the retention indices of organic compounds on GDX-1, -2 and -3 were similar, they were considered to be non-polar stationary phases according to Kováts empirical rule[5]. The elution of polar compounds with similar boiling points in order of decreasing polarity seemed to be further evidence. However, GDX-303, which was best suited for the analysis of sulphur compounds, interacted more or less with water and alcohol. The retention of water is rather long with a tailing peak and the separation is poor. This indicates that GDX-3 is slightly more polar than GDX-1 and -2.

The weakly basic functional groups in GDX-4 make it somewhat polar. The retention of cyclohexane is smaller than that of benzene because of the polarizable π-bond in the latter. The order of elution of C_2 olefins is ethylene–acetylene–ethane compared with ethylene–ethane–acetylene on GDX-1. Probably the functional groups account for the outstanding separation of water from hydrogen chloride and from ammonia.

The strongly polar functional groups in GDX-5 make its chromatographic behaviour distinctly different from that of the above two types. The order of elution of many substances on GDX-5 are the reverse of that on the non-polar GDX packings, *e.g.*, diethyl ether, with a smaller dipole moment (1.17 D), elutes faster than ethanol (1.73 D) and benzene is selectively retained owing to its π-electrons. The retention times of those compounds with larger dipole moments, such as methyl cyanide and nitro compounds, are much longer than those of *n*-alkanes on GDX-5. The C_2 olefins can be resolved completely on GDX-502 at room temperature, the elution order being the same as that on GDX-4. These results lead to the conclusion that GDX-5 is strongly polar.

Preliminary research on the separation mechanism of GDX

Elucidation of the separation mechanism of porous polymer beads used as GC packings was attempted in several ways. The question of whether the dominating process in the separation is adsorption, solution or both has been posed for a long time. Barte and Gorden[6], who support an adsorption mechanism, suggested that there are active centres on Porapak Q with which the α-hydrogen of ketones can exchange. According to the well known phenomenon of gas molecules penetrating the skeleton of polymer, Tranchant[7] considered that dissolution would be the major process except when the solute molecules are inhibited on the surface by a noticeable difference in polarity.

We[8] have studied the relationship between the retention volume (V_g) and the specific surface area (σ) of C_4 olefin isomers on GDX-5, and tried to find the contribution of each process.

Assuming the additivity of adsorption and solubility processes, we have

$$V_R = V_d + S\gamma + W\beta \tag{1}$$

where V_R is the relative retention volume, V_d the gas phase volume in the column, γ the adsorption coefficient, β Henry's coefficient, and S and W the surface area and mass of the sorbent in the column, respectively. We can rewrite eqn. 1 as

$$V'_R = V_R - V_d = S\gamma + W\beta \tag{2}$$

and

$$V_s = V'_R/S = \gamma + \beta/\sigma \tag{3}$$

where σ is the specific surface area of the sorbent. Using sorbents of the same chemical composition but different porosity, β and γ are obtained from the slopes and intercepts of the V_S *versus* $1/\sigma$ lines respectively, as shown in Fig. 3.

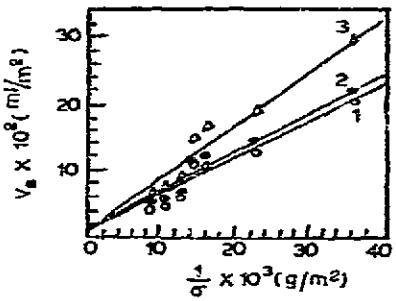

Fig. 3. V_s versus $1/\sigma$ relationship of some C_4 olefins. $T_c = 108°$. 1 = Isobutene; 2 = *trans*-butene-2; 3 = butadiene-1,3.

The results of our experiments show that: (1) adsorption coefficients (γ) are small compared with solubility coefficients (β); (2) for olefins, the larger the molecular polarizabilities the larger are their γ values; this is in agreement with the principle of interaction between adsorbed molecules and the surface of the sorbent; (3) the retention volume increases with increasing β for all of the components tested. We found that Henry's coefficients for C_4 olefins contribute to the retention to the extent of nearly 90%, and adsorption coefficients only to 10%. This means that solute molecules penetrate deeply into the skeleton of the polymer network and thus the solution mechanism seems to be predominant, at least as far as the above-described system is concerned.

TDX POROUS CARBON BEADS FOR GC

Kaiser[9] used poly(vinylidene chloride) (PVDC) as a precursor of porous carbon in 1969. This kind of pure carbon material possesses a highly inert surface similar to that of graphite. Water elutes from it even earlier than methane. In our laboratory, PVDC beads were first synthesized by suspension polymerization, and then underwent controlled pyrolytic decomposition to porous carbon beads. This kind of sorbent is now commercially available under the name TDX-01. It has outstanding features in analysing rare and permanent gases, light olefins, etc., under convenient chromatographic conditions[10]. In this work, emphasis is placed on further treatment of these beads at high temperature under a pure hydrogen atmosphere to eliminate the residual active groups on the surface, and the product was named TDX-02. Water elutes with a sharp, symmetrical peak and hence it is extremely useful in the trace analysis of water. One drawback may be the liability of its becoming contaminated with high-boiling compounds. Fortunately, GDX and TDX are complementary to each other. The combined use of TDX and GDX has solved a wide variety of problems in analysing trace amounts of water in various organic substances.

Preparation of porous carbon beads

Synthesis. PVDC was prepared by suspension polymerization using a compound dispersant at 40°. The beads obtained were washed with water and acid

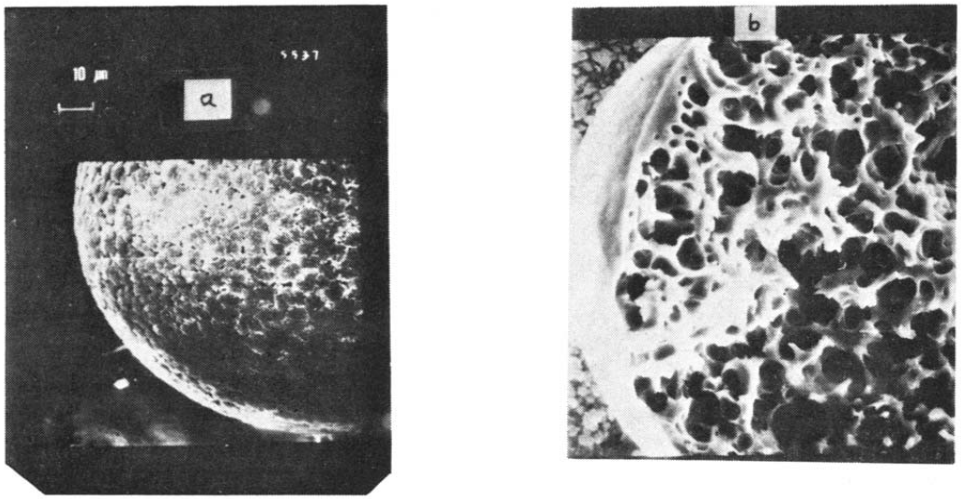

Fig. 4. SEM of TDX under (a) controlled and (b) uncontrolled rate of carbonization.

alternately; care should be taken to avoid contamination by iron (*III*) ions. The beads were then extracted with an organic solvent, dried and sieved.

Pyrolysis. The first stage of pyrolysis began at 180°, which should be carried out in a gradual manner to ensure that no clustering will occur. Boult *et al.*[11] indicated that such carbon chips were essentially non-graphitized but had a high surface area and micropores. From a topographical study by scanning electron microscopy (SEM) during gasification, it was found that the physical change in the pore structure depends directly on the rate of carbonization and the particle size of the PVDC chips. Our experimental results for pyrolysis at different rates are shown in Fig. 4a and b. It is believed that the rate of escape of hydrogen chloride determines the pore structure. A "phase" transition at 300–400°, as shown in Fig. 5,

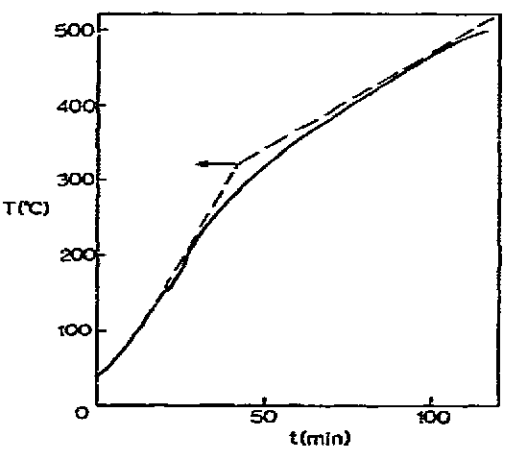

Fig. 5. "Phase" transition during pyrolysis of poly(vinylidene chloride). Home-made muffle, pyrolysis at 3.8 A, 190 V.

was found for a heating rate of 4°/min under a stream of argon. This agreed well with Boult *et al.*'s result in which carbon passed through a plastic stage where the amount of evolution of hydrogen chloride reached a maximum. The "phase" transition zone was supposed to be the second stage, the key stage in which the viscous aggregates were forced apart by the evolved hydrogen chloride. After this, the temperature was increased at a rate of 5°/min and then maintained at 400° until hydrogen chloride was undetectable at the outlet of the pyrolysis tube. The same was done at 600°, 800°, 1000° and 1200°. The specific surface areas of these carbon beads increase with carbonization temperature as shown in Fig. 6. The column efficiency was improved gradually after the inflexion point at 600°. To obtain a pure carbon skeleton in the shortest possible time a pyrolysis temperature of 900–1000° is preferred. An after-treatment involving high-temperature reduction in a pure hydrogen atmosphere yielded sorbents of superior performance, on which water eluted before methane, as shown in Fig. 7.

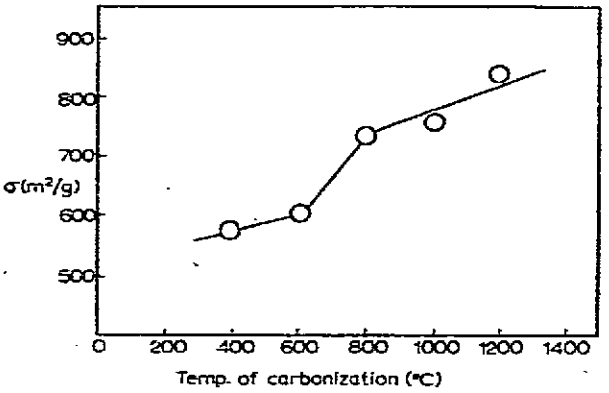

Fig. 6 Effect of temperature of carbonization on specific surface area

Fig. 7. Separation of water and methane. Column: 1 m × 3 mm I.D. TDX-02. T_c = 120°; I_b = 180 mA; hydrogen flow-rate = 55 ml/min. 1 = Air (25 sec); 2 = water (58 sec); 3 = methane (1 min 18 sec).

Investigation on some properties of porous carbon beads

The advantage of PVDC as a carbon precursor is its regular crystalline structure and the absence of large amounts of heteroatoms other than chlorine. During pyrolysis, hydrogen chloride molecules evolved easily and the carbon chains rearranged to a stable, low energy level. These porous carbons are sometimes named molecular sieves, but Patzelova[12] stated that it belongs to the first type of adsorbent according to Kiselev's classification. From the author's point of view, as TDX already possesses a homogeneous microporous structure with a large specific surface area, its surface properties should be the essential factor in determining the chromatographic performance[13]. In the separation of common gases, TDX behaves like molecular sieves where the order of elution follows the size of the gas molecules;

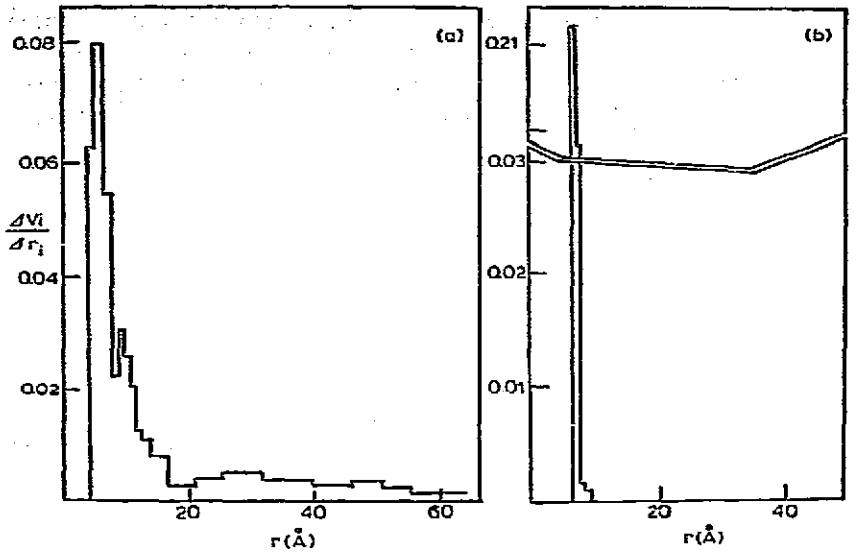

Fig. 8. Pore-size distribution of (a) activated carbon and (b) TDX.

however, in the separation of polar compounds, the effect of the surface character becomes predominant. The residual active groups on the TDX-01 surface give a tailing peak for water which makes it unsuitable for trace water analysis.

EPR and small-angle X-ray scattering studies showed that TDX is non-graphitized. However, the pore size distribution and EPR results are different from those for activated carbon, as shown in Fig. 8a and b. From a plot of $\log V_g$ *versus* $1/T$ for water, methane and carbon dioxide on TDX-01 and -02 (Fig. 9), it can be

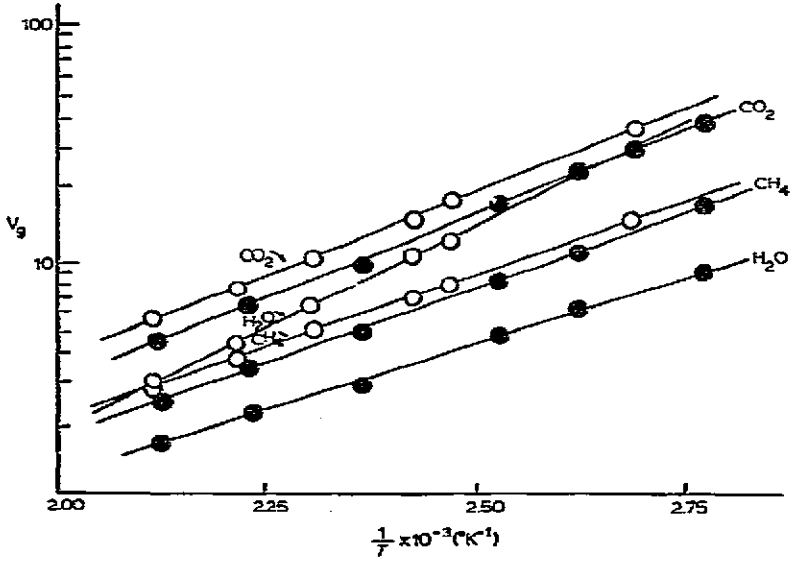

Fig. 9. Relationship between retention and temperature for TDX-01 (○) and TDX-02 (●).

seen that the slopes of all of the lines are nearly the same except for that of water on TDX-01. Water usually elutes after methane on TDX-01 until a definite temperature (*ca.* 180°) is exceeded. Further, the difference between the adsorption properties of water on these two TDXs can be shown by the following equation. As

$$\ln \overline{V}_g = -\Delta H/RT + \Delta S/R$$

we must have

$$\Delta H_{TDX\text{-}01} > \Delta H_{TDX\text{-}02}$$

and

$$\Delta S_{TDX\text{-}01} < \Delta S_{TDX\text{-}02}$$

The heats of adsorption of TDXs were studied kinetically by means of a microcalorimeter. Fig. 10 shows the differential heat of adsorption of water and the mass of water adsorbed on TDXs. The experimental results under isothermal, isobaric and equi-surface area conditions were as follows:

$$\int(\mathrm{d}\Delta H/\mathrm{d}t)_{TDX\text{-}01}\mathrm{d}t > \int(\mathrm{d}\Delta H/\mathrm{d}t)_{TDX\text{-}02}\mathrm{d}t$$

$$(\mathrm{d}^2\Delta H/\mathrm{d}t^2)_{TDX\text{-}01} > (\mathrm{d}^2\Delta H/\mathrm{d}t^2)_{TDX\text{-}02}$$

in most instances, and

$$\Delta m_{TDX\text{-}01} < \Delta m_{TDX\text{-}02}$$

From these results, the following conclusions can be drawn:

(1) water is more tightly bound to TDX-01 than to TDX-02;

(2) there are more active centres on TDX-01 than on TDX-02;

(3) from the magnitude of entropy decrease, TDX-02 adsorbs water molecules more regularly than TDX-01 does;

(4) parallel to (3), more water can be adsorbed on TDX-02 than on TDX-01.

The presence of active centres in TDX-01 is evident and this stresses the importance of after-treatment of TDX-01. The "graphite"-like surface makes TDX-02 an excellent packing material for use in the trace analysis of water.

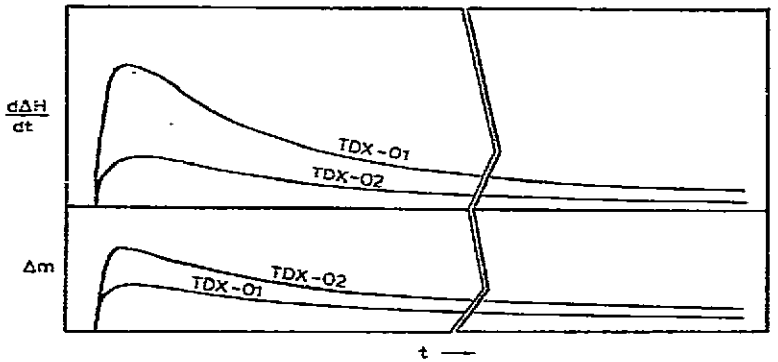

Fig. 10. Effect of heat of adsorption on TDX.

Applications of GDX and TDX sorbents in GC

Trace analysis of water. This is an important but difficult problem to solve in research and industry. Figs. 11a and b show the routine determination of corrosive materials in industry by GC. The trace analysis of water in pure butadiene is easily accomplished with GDX if the separation between water and C_2 and C_3 hydrocarbons is not considered. If TDX-02 is used, the separation is satisfactory with a sensitivity of 4–10 mm peak height per 1 ppm. An on-line analysis is shown in Fig. 12[14,15].

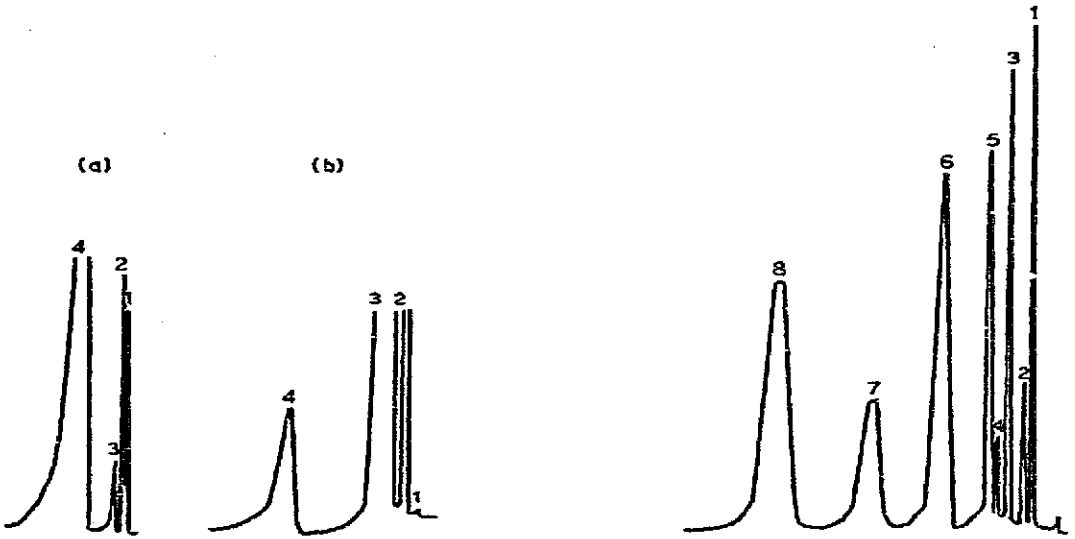

Fig. 11. (a) Chromatogram of water and hydrogen chloride. Column: 1.6 m × 4 mm I.D. GDX-401. T_c = 108°; I_b = 190 mA; hydrogen flow-rate = 17.8 cm/sec. 1 = Air (9.2 sec); 2 = C_2H_2 (14.2 sec); water (51.4 sec); 4 = hydrogen chloride (2 min 45 sec). (b) Determination of trace amounts of water in hydrogen sulphide. Column: 2 m × 4 mm I.D. GDX-403. $T_c = T_d$ = 80°; hydrogen flow-rate = 70 ml/min; gold-plate TCD, 200 mA. 1 = Air (18 sec); 2 = carbon dioxide (23 sec); 3 = hydrogen sulphide (29 sec); 4 = water (2 min 25 sec).

Fig. 12. Determination of trace amounts of water in butadiene or isoprene. Column: 0.8 m × 3 mm I.D. TDX-02. T_c = 118°; P_i (N_2) = 1.0 kg/cm²; I_b = 100 mA. 1 = Helium (9.7 sec); 2 = air (24 sec); 3 = methane (54 sec); 4 = water (1 min 18 sec); 5 = carbon dioxide (1 min 35 sec); 6 = acetylene (3 min 16 sec); 7 = ethylene (5 min 43 sec); 8 = ethane (8 min 50 sec).

Analysis of gases. Gases (H_2, O_2, Ar, N_2, CO_2, CH_4, etc.) dissolved in underground water or over deserted wells sometimes provide useful information in the prediction of a forthcoming earthquake. It is, however, often difficult to determine the gas composition quantitatively. Using palladium coated TDX-02 to transform oxygen into water[16], argon and oxygen can be determined simultaneously in addition to other gas components (Fig. 13). Other examples are the detection of latent faults in power transformers, as shown in Fig. 14, and the analysis of high-purity helium, as shown in Fig. 15a and b.

Automatic monitoring of air pollutants. This was carried out on a moveable base[17]. GDX and TDX were satisfactory for determining methane, acetylene,

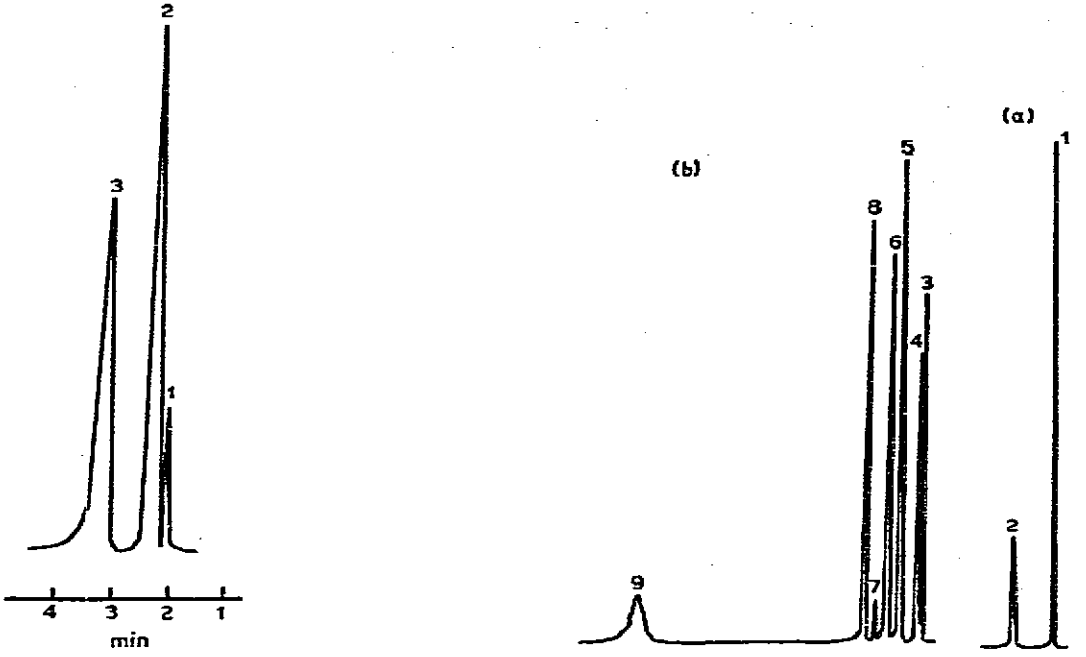

Fig. 13. Separation of inert gases. Columns: 2 m × 3 mm I.D. TDX-01 and 0.2 m × 3 mm I.D. TDX-02-Pd (catalytic column). Hydrogen flow-rate = 80 ml/min; I_b = 150 mA.

Fig. 14. Determination of gases from a certain part of a faulty transformer. (a) Column, 1 m × 2 mm I.D. TDX-01; T_c = 38°; nitrogen flow-rate = 34 ml/min. (b) Column, 2 m × 3 mm I.D. GDX-502; T_c = 38°; nitrogen flow rate = 29 ml/min. 1 = Hydrogen (25 sec, 1.11%); 2 = oxygen (1 min 48 sec, 16.6%); 3 = carbon monoxide (36 sec, 0.042%); 4 = methane (43.7 sec, 0.43%); 5 = carbon dioxide (1 min 22 sec, 2.0%); 6 = ethylene (1 min 54 sec, 0.56%); 7 = acetylene (2 min 23 sec, 0.0048%); 8 = ethane (2 min 46 sec, 1.59%); 9 = propene + propane (11 min 9 sec).

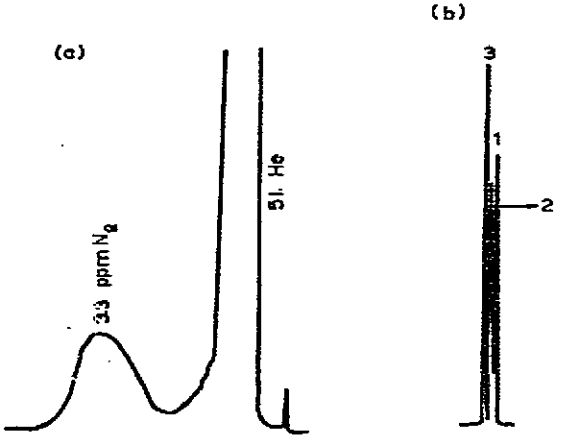

Fig. 15. (a) Impurity in high-grade helium. (b) Separation of helium, neon and hydrogen. Column: 2 m × 3 mm I.D. TDX-01. T_c = 50°; I_b = 150 mA; nitrogen flow-rate = 43 ml/min. 1 = Helium (31.3 sec); 2 = neon (36.5 sec); 3 = hydrogen (49 sec).

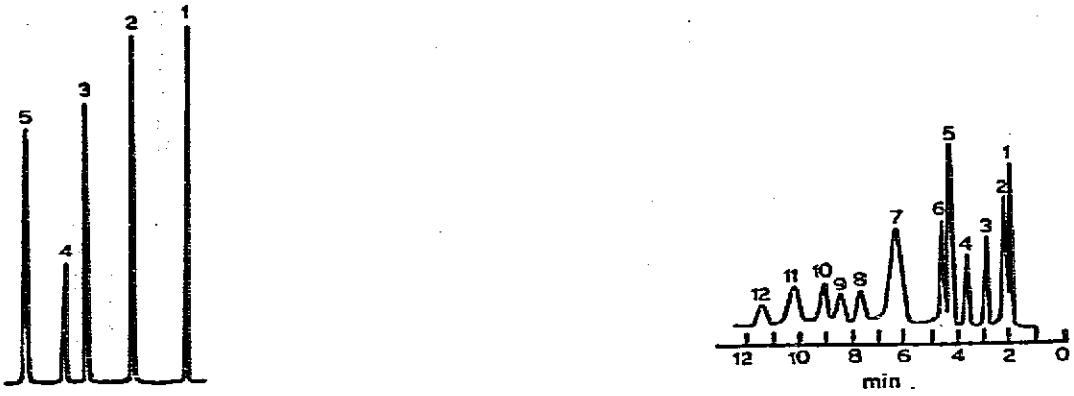

Fig. 16. Determination of the four air pollution components. Column: 1 m × 3 mm I.D. TDX-02 and 5 m × 3 mm I.D. GDX-502. $T_c = 50°$; $T_i = 370°$; FID; hydrogen flow-rate = 50 ml/min. 1 = Total hydrocarbons ($K = 81$), 30 ppm; 2 = methane ($K = 2$), 10 ppm; 3 = ethylene ($K = 1$), 10 ppm; 4 = acetylene ($K = 1$), 10 ppm; 5 = carbon monoxide ($K = 1$), 10 ppm.

Fig. 17. Separation of C_1–C_4 olefins on GDX-501 (70–90 mesh). Column: 6 m × 3 mm I.D. $T_c = 108°$; $I_b = 200$ mA; hydrogen flow-rate = 19 ml/min. 1 = Air; 2 = methane; 3 = ethylene + ethane; 4 = acetylene; 5 = propane; 6 = propene; 7 = isobutane; 8 = *n*-butane; 9 = isobutene; 10 = *trans*-butene; 11 = *cis*-butene; 12 = butadiene-1,3.

ethylene, carbon monoxide and total hydrocarbons, the period of analysis being about 15 min (Fig. 16).

Analysis of purity of raw materials in industry. The separation of C_4 hydrocarbons on GDX-501 is shown in Fig. 17. The analysis of the raw materials of Orlon, poly(methyl methacrylate) and the dimer of cyanogen chloride are shown in Figs. 18, 19 and 20, respectively.

YSG POLYMERIC MICROSPHERES FOR LC

Intensive studies on high-efficiency column packings and instrumentation led to a breakthrough in modern LC in 1969. The development of controlled surface porosity packings and totally porous siliceous microspheres and synthetic polymeric microspheres produced by Hitachi[18] led to major successes in high-performance liquid chromatographic analysis and in preparative separations such as enrichment and purification. Generally cross-linked polystyrene copolymer can be used as basic materials for the synthesis of polymer sorbents.

Two kinds of polymeric stationary phase for LC have been synthesized and studied in our laboratory: (1) ethylstyrene–divinylbenzene copolymers and (2) cross-linked polystyrene ion-exchange resin microspheres.

Ethylstyrene–divinylbenzene microspheres

Spherulitization and fundamental properties. A strictly spherical shape and a suitable porosity are desirable for LC packings. In our laboratory, microbeads (<20–30 μm) were prepared by suspension–emulsion polymerization in a saturated "ivory" soap solution with gentle stirring. The copolymer latex itself acted as a dispersant, as shown in Fig. 21. The particle size depended mainly on the rate of stirring,

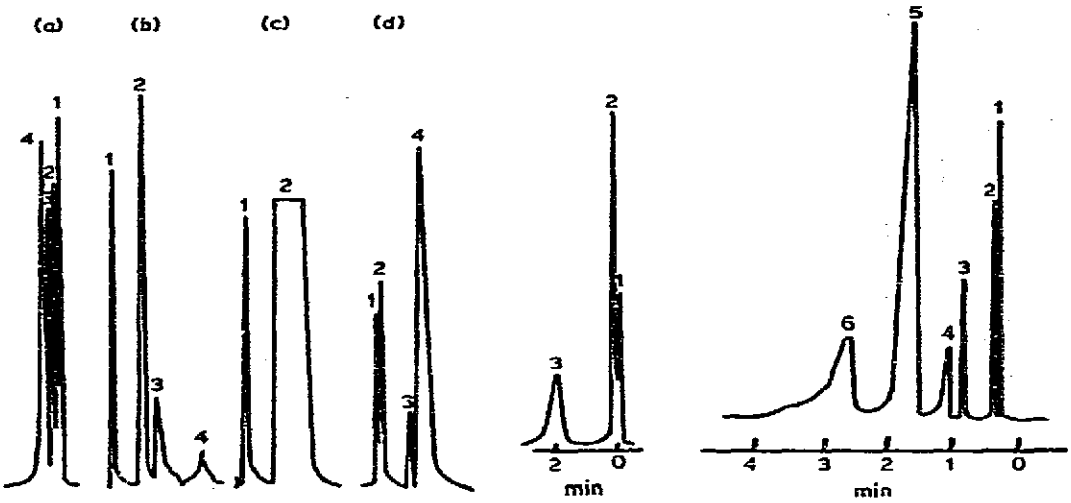

Fig. 18. Determination of acrylonitrile and its impurities. (a) Raw gases. Column: 1 m × 3 mm I.D. GDX-401. T_c = 105°; I_b = 150 mA; hydrogen flow-rate = 30 ml/min. 1 = Air (38.2 sec); 2 = ammonia (1 min 10 sec); 3 = pentene (1 min 31 sec); 4 = water (2 min 45 sec). (b) Four-component mixture. Column: 1 m × 3 mm I.D. GDX-102. T_c = 120°; I_b = 150 mA; hydrogen flow-rate = 30 ml/min. 1 = Water; 2 = methyl cyanide; 3 = acrylonitrile; 4 = ethyl cyanide. (c) Water in acrylonitrile. Conditions as in (b). 1 = Water; 2 = acrylonitrile. (d) Raw acrylonitrile. Conditions as in (b). 1 = Water; 2 = hydrogen cyanide; 3 = methyl cyanide; 4 = acrylonitrile.

Fig. 19. Determination of impurities in acetone cyanohydrin and its impurities. Column: 1 m × 4 mm I.D. GDX-102. T_c = 100°; nitrogen flow-rate = 40 ml/min. 1 = Water; 2 = hydrogen cyanide; 3 = acetone.

Fig. 20. Separation of corrosive gases. Column: 3 m × 3 mm I.D. GDX-103–GDX-401 (2:1, v/v). T_c = 85°; T_d = 100°; T_v = 110°; I_b = 200 mA; hydrogen flow-rate = 353 ml/min. 1 = Air; 2 = carbon dioxide; 3 = cyanogen; 4 = water; 5 = cyanogen chloride; 6 = chlorine + hydrogen chloride.

which was controlled within the range 200–600 rpm. The gelation time must be controlled strictly and an additional portion of soap solution was added to prevent coagulation if necessary. A high degree of cross-linking was needed and a good solvent was used as the diluent. The commercial name of this packing is YSG-01.

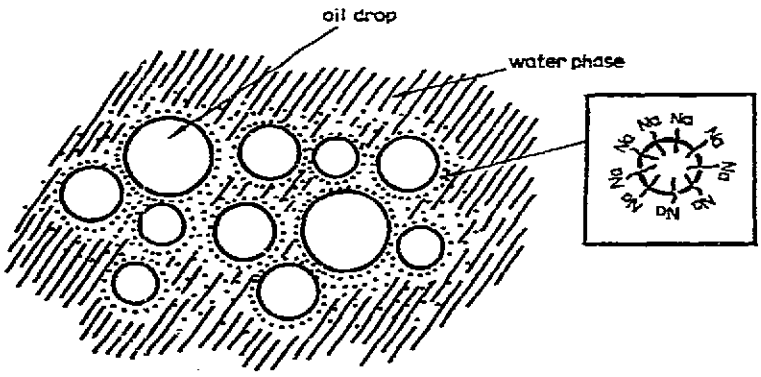

Fig. 21. Scheme of suspension–emulsion polymerization.

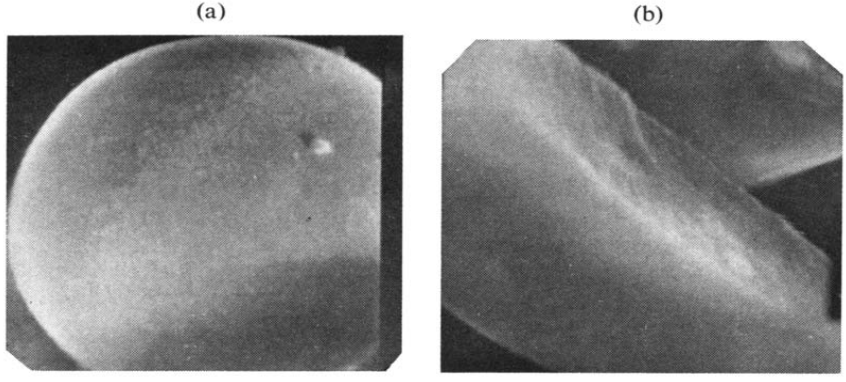

Fig. 22. SEM of (a) exterior (×5000) and (b) interior (×2500) surface of YSG-01.

The SEM investigation of its exterior and interior surfaces are shown in Fig. 22a and b, respectively. The specific surface area and pore size distribution were determined by the dual gas channel flow method[19]. The specific surface area of YSG-01 is about 300 m^2/g under nitrogen (77° K), and from the pore size distribution curve shown in Fig. 23, the average pore diameter is approximately 50 Å. This value is comparable to the 80 Å obtained by gel permeation chromatography using tetrahydrofuran (THF) as solvent.

Sieving of non-polar polymeric microspheres. The sieving of these electrostatic and hydrophobic microspheres was carried out through a flow of pressurized alcohol under ultrasonic vibration. Micro-mesh sieve cloths with different mesh sizes were

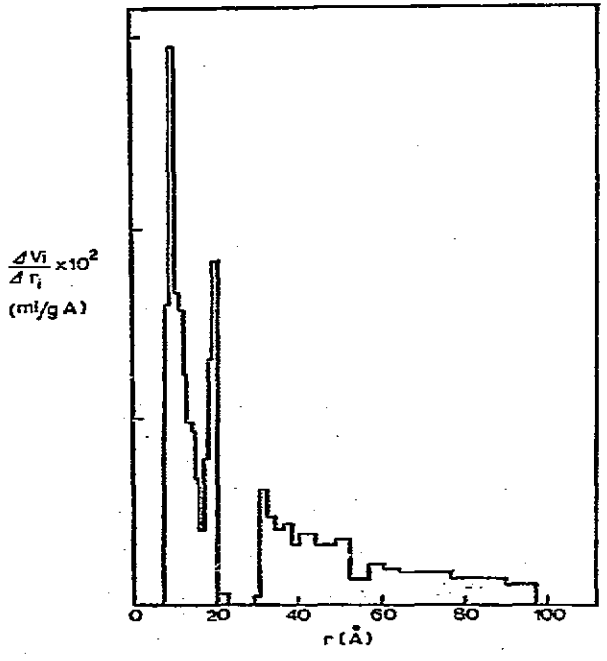

Fig. 23 Pore-size distribution of YSG-01.

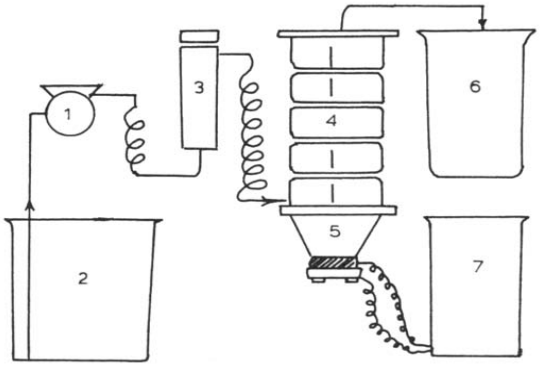

Fig. 24. Sieving under ultrasonic vibration. 1 = Pump; 2 = liquid tank; 3 = feed can; 4 = micropore sieve plate column; 5 = ultrasonic generator; 6 = filtered liquid tank; 7 = ultrasonicator.

produced by nickel plating of common copper wire gauze for different plating periods. The apparatus is shown in Fig. 24. Fractions of 25–30, 22–25 and 18–22 μm were microphotographed as shown in Fig. 25.

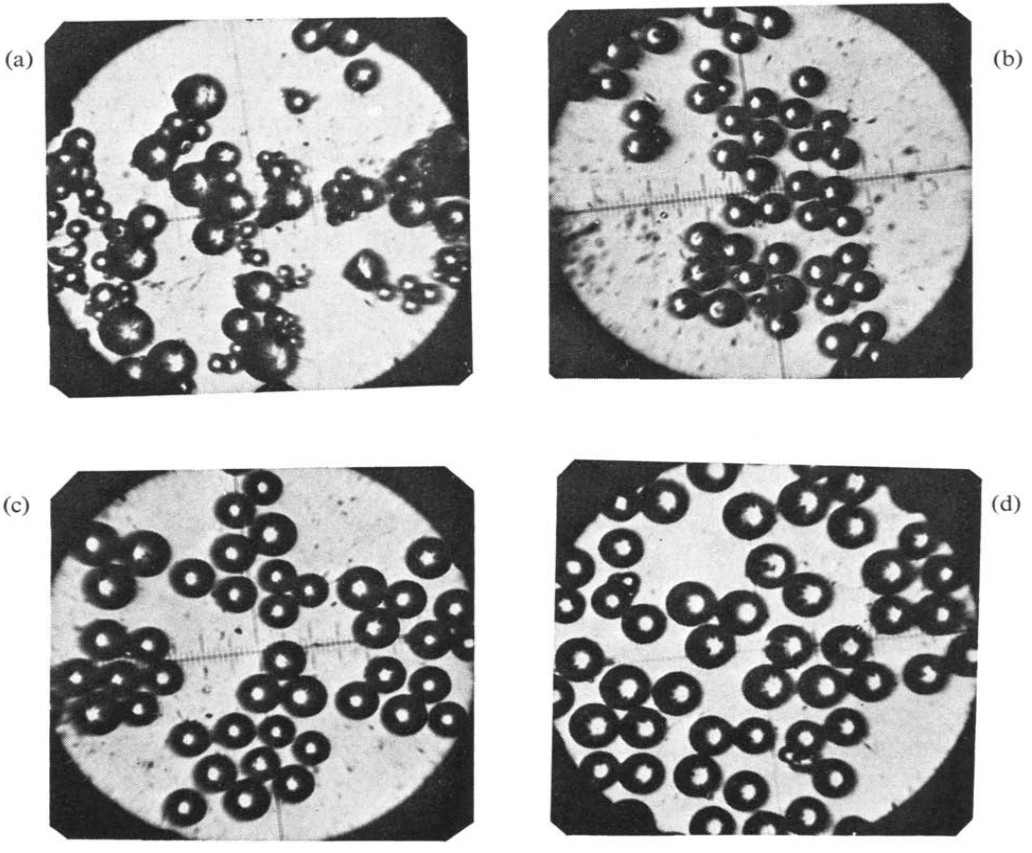

Fig. 25. Microphotograph of YSG-01 fractions. (a) Polydisperse; (b) 18–22 μm; (c) 22–25 μm; (d) 25–30 μm.

Some fundamental properties of YSG-01 are summerized in Table III.

TABLE III

SOME FUNDAMENTAL PROPERTIES OF YSG COLUMNS

Property	*Column*		
	*YSG-01**	*YSG-$SO_3^-Na^+$**	*YSG-$CH_2N^+(CH_3)_3Cl^-$**
Specific surface area (m^2/g)	300	2	2
Average particle diameter (Å)	51, 80**	—	—
Pore capacity (ml/g)	1.8**	—	—
Packing density (g/ml)	0.4–0.5	0.5–0.6	0.5–0.6
Colour	White	Pale yellow	Slight yellow
Columa efficiency (number of plates per metre)***	1000[a] (<35 μm) 1270 (18–22 μm)	400[b] (<35 μm) 2000 (10–15 μm)	200[c] (<35 μm) 860 (15–25 μm)%
Sample capacity (ml/g)***	*ca.* 8[a]	—	—
Water content (%)	—	58 ± 2	48–54
Ion-exchange capacity (mequiv./g, dry)	—	5.0 ± 0.2	*ca.* 3.8
Fractions (μm)	18–22	10–15	10–15
	22–25	15–20	15–25
	25–30	20–25	—

* The YSG columns correspond to the Hitachi series[20] as follows: YSG-01, Hitachi 3010; YSG-$SO_3^-Na^+$, Hitachi 2610; YSG-$CH_2N^+(CH_3)_3Cl^-$, Hitachi 2631.

** Determination according to Van Kreveld and Van den Hoed[21].

*** Chromatographic conditions and samples for a, b and c: (a) Perkin-Elmer LC-1220, 250 × 2.6 mm I.D. column; 25°; detection, UV, 254 nm; eluent, methanol; sample, N-methylaniline. (b) Perkin-Elmer LC-1220; 250 × 2.6 mm I.D. column; eluent, 0.5 *M* ammonium acetate, pH 6; 70°; detection, UV, 254 nm; sample, cytidine. (c) Hitachi 635 LC; 150 × 2.1 mm I.D. column; eluent 0.3 *M* NaCl–0.01 *M* HCl, pH 2.13; 60°; detection, refractive index; $R = 2 \cdot 10^{-6}$; sample, ADP.

Chromatographic characteristics of YSG-01. (1) Swelling properties: swelling or shrinking of the beads is detrimental, especially in gradient elution, so the swelling indices of YSG-01 in different solvents were determined (see Table IV).

(2) Relationship between column efficiency and linear velocity of eluent: this generally conforms to the following equation:

$$H = Ku^n$$

where n characterizes the stationary phase mass transfer and lies between 0.2 and

TABLE IV

SWELLING PROPERTIES OF YSG IN VARIOUS SOLVENTS

Determined at 30°; methanol used as relative standard.

	Methanol–water					*Acetone*	*Chloroform*	*Isooctane*
	100:0	*90:10*	*70:30*	*50:50*	*30:70*			
Relative degree of swelling	1.0	0.96	0.91	0.88	0.75	1.00	1.01	1.08

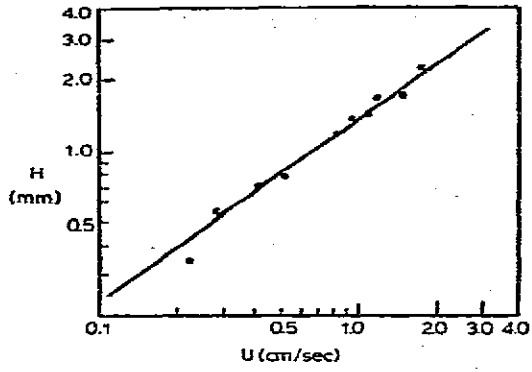

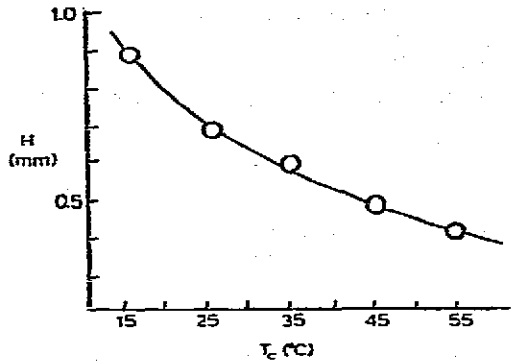

Fig. 26. Relationship between HETP and linear eluent velocity. $T_c = 25°$; eluent, methanol; sample, N-methylaniline.

Fig. 27. Relationship between HETP and column temperature. Eluent, methanol; sample, N-methylaniline.

0.8. As shown in Fig. 26, $n = 0.78$ for YSG-01, which means that the mass transfer resistance is still large.

(3) Relationship between column efficiency and temperature: the temperature dependence of the diffusion factor of solute molecules in the polymer is well defined. If the column temperature is suitably raised, the column efficiency will be improved (Fig. 27).

(4) Influence of mobile phase composition on resolution: variation of mobile phase composition greatly increases the separation capability. Fig. 28 presents two examples.

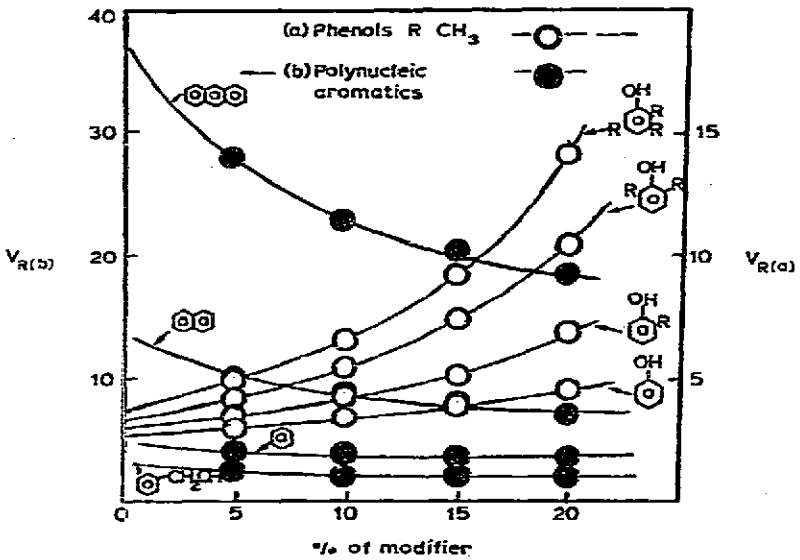

Fig. 28. Mixed solvent effect on retention. (a) Water in methanol; (b) isooctane in methanol. $T_c = 25°$; flow-rate, 1 ml/min.

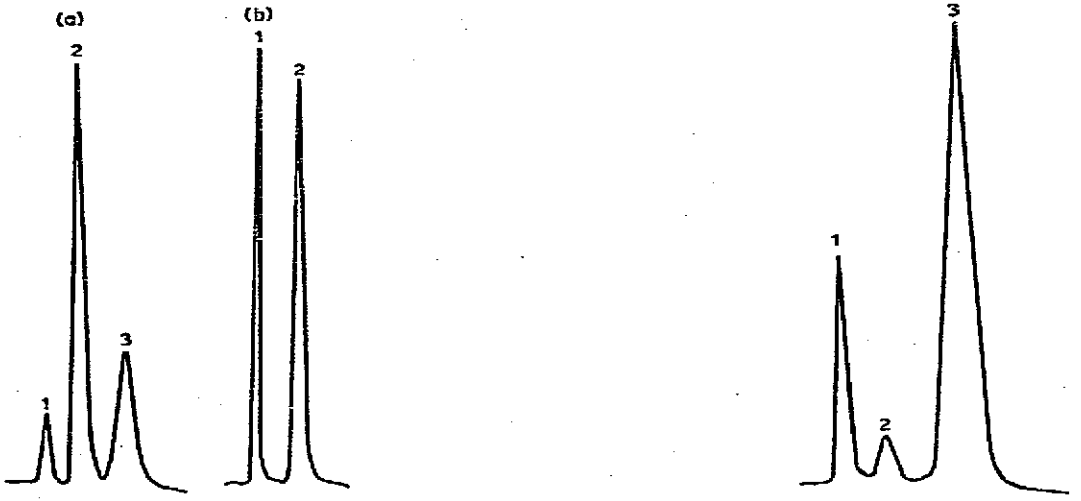

Fig. 29. Separation of drugs. Column: 500 × 2.6 mm I.D. YSG-01; eluent, methanol; flow-rate, 1 ml/min; detection: UV, 254 nm, 0.1 O.D.; room temperature. (a) 1 = Aspirin (1 min 40 sec); 2 = phenacetin (3 min 20 sec); 3 = caffeine (5 min 31 sec). (b) 1 = Sulpyrine (1 min 41 sec); 2 = aminopyrine (3 min 49 sec).

Fig. 30. Separation of steroids. Conditions as in Fig. 29, except temperature, 50°. 1 = Oestradiol (3 min 27 sec); 2 = oestrone (5 min 35 sec); 3 = progesterone (9 min 10 sec).

Applications. YSG-01 is recommended for the separation of polar aromatics, polynuclear aromatics, dyestuff intermediates, plasticizers and pharmaceuticals. It is especially useful for the rapid determination of steroids, and two examples are shown in Figs. 29 and 30.

Cross-linked polystyrene ion-exchange resin microspheres

A strong cation-exchange (SCX) and an anion-exchange (SAX) resin were prepared, with commercial names YSG-SO_3H and YSG-$CH_2N^+(CH_3)_3Cl^-$, respectively. The fundamental properties of these microspheric resins are given in Table III.

Particle size fractionation of the resins was effected by sedimentation in water and alcohol for SCX and SAX, respectively. The glass vessels should be silanized in order to avoid adsorption on the glassware. The particle size distribution evidently affects the column efficiency, as shown in Table V.

TABLE V

RELATIONSHIP BETWEEN RESIN PARTICLE SIZE AND EFFICIENCY

Conditions: Perkin-Elmer LC-1220; column, 250 × 2.6 mm I.D.; eluent, 0.5 *M* ammonium acetate, pH 6; detection, UV, 254 nm. Efficiency is given as the number of plates for CMP (N_{CMP}) at 70°, and for tryptophan (N_{Trp}) at 60°.

Diameter of resin (μm)	N_{CMP}	N_{Trp}
5–30	99	87
15–20	243	228
10–15	505	443

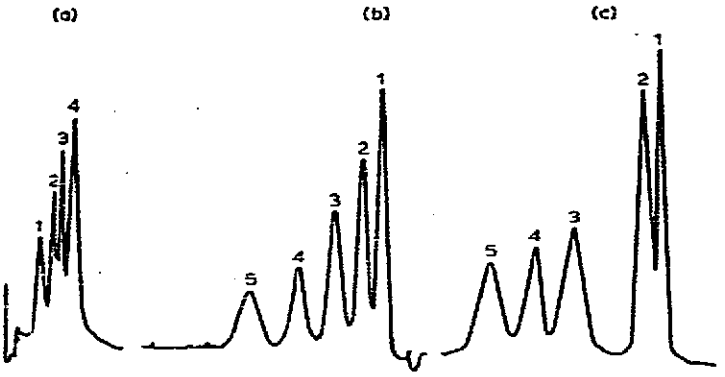

Fig. 31. Separation of mono- and dibasic organic acids. (a) Column: 100 × 9 mm I.D. YSG-SO_3H. Eluent, water; flow-rate, 1 ml/min; temperature, 50°; Coulomb potentiometer. 1 = Formic acid (6 min 21 sec); 2 = acetic acid (7 min 22 sec); 3 = propionic acid (8 min 12 sec); 4 = butanoic acid (9 min 15 sec). (b) Column: 100 × 9 mm I.D. in series YSG-SO_3H. Eluent, methyl cyanide–water (20:80); flow-rate, 1 ml/min; Ag–C electrode, 0.45 V Ag–AgI. 1 = Hexanoic acid (14 min 30 sec); 2 = heptanoic acid (16 min 17 sec); 3 = octanoic acid (18 min 50 sec); 4 = nonanoic acid (22 min 18 sec); 5 = decanoic acid (27 min). (c) Column: 500 × 9 mm I.D. YSG-SO_3H. Eluent, water; flow-rate, 1 ml/min; temperature, 48°; Coulomb potentiometer. 1 = Ethanedicarboxylic acid; 2= propanedicarboxylic acid; 3 = butanedicarboxylic acid; 4 = pentanedicarboxylic acid; 5=hexanedicarboxylic acid.

Applications of SCX and SAX in the analysis of organic acids, nucleosides, amino acids, adenosine phosphates and the rapid separation of tungsten and molybdenum in high-alloy steel, etc., are shown in Figs. 31–34.

Studies on the dependence of chromatographic behaviour on the pore structure of the polymer are in progress.

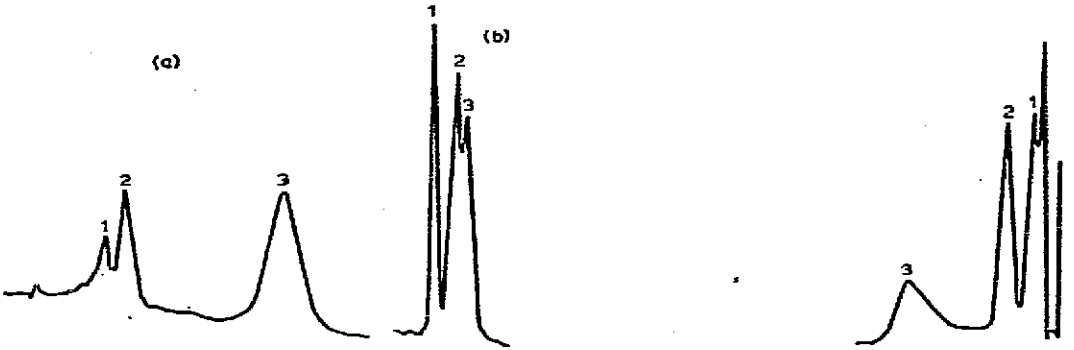

Fig. 32. Separation of (a) amino acids and (b) nucleosides. Column: 250 × 2.6 mm I.D. YSG-SO_3H. Eluent, 0.5 *M* ammonium acetate, pH 6; detection, UV, 254 nm. (a) Flow-rate, 0.46 ml/min; 60°. Peaks: 1 = tyrosine (4 min 55 sec); 2 = phenylalanine (5 min 54 sec); 3 = tryptophan (13 min 43 sec). (b) Flow-rate, 0.4 ml/min; 70°. Peaks: 1 = uridine (2 min 59 sec); 2 = guanosine (3 min 53 sec); 3 = adenosine (4 min 22 sec).

Fig. 33. Separation of adenosine phosphates. Column: 150 × 2.1 mm I.D. YSG-$CH_2N^+(CH_3)_3Cl^-$. Eluent, 0.3 *M* NaCl–0.01 *M* HCl, pH 2.13; flow-rate, 0.7 ml/min; temperature, 60°; detection, refractive index. Peaks: 1 = AMP (1 min 15 sec); 2 = ADP (2 min 40 sec); 3 = ATP (7 min 27 sec).

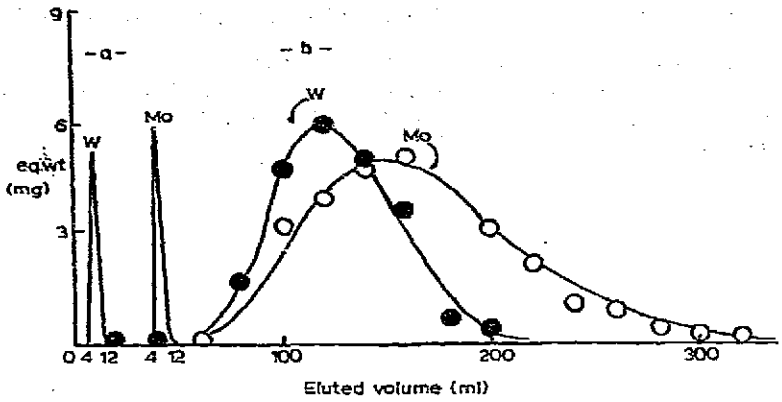

Fig. 34. Determination of tungsten and molybdenum in high-alloy steel. Eluents: for tungsten, 10% hydrofluoric acid–60% hydrochloric acid; for molybdenum, 20% hydrofluoric acid–25% hydrochloric acid. Column: (a) YSG-$CH_2N^+(CH_3)_3Cl^-$ (20–50 μm); (b) ion-exchange resin 801 (16–80 mesh).

ACKNOWLEDGEMENTS

The author acknowledges the contribution of her collaborators in the Chromatography Group of the Institute of Chemistry and the cooperation of the Second Chemical Reagent Manufacturing Factory, Tientsin. The author also thanks Prof. S. C. Liang for reviewing the manuscript, Professors Y. H. Sha and Zhu An for helpful discussions in writing this paper and Mr. R. S. Li for his assistance in taking the photographs.

REFERENCES

1 O. L. Hollis, *Anal. Chem.*, 38 (1966) 308.
2 Chromatography Group of the Institute of Chemistry, Academia Sinica, *Fenxi Huaxue*, 1 (1973) 244.
3 J. C. Moore, *J. Polym. Sci., Part A*, (1964) 835.
4 Chromatography Group of the Institute of Chemistry, Academia Sinica, *Huaxue Yenjiu*, 1 (1977) 38.
5 E. Sz. Kováts, *Advan. Chromatogr.*, 1 (1965) 229.
6 C. I. Barte and A. S. Gorden, *J. Chromatogr. Sci.*, 8 (1970) 63.
7 J. Tranchant, *Z. Anal. Chem.*, 236 (1968) 137.
8 Chromatography Group of the Institute of Chemistry, Academia Sinica, *Fenxi Huaxue*, 3 (1975) 188.
9 R. Kaiser, *Chromatographia*, 2 (1969) 453.
10 Chromatography Group of the Institute of Chemistry, Academia Sinica, *Huaxue Tongbao*, 3 (1975) 30.
11 E. H. Boult, H. G. Campbell and H. Marsh, *Carbon*, 7 (1969) 700.
12 V. Patzelová, O. Kadlec and P. Seidl, *J. Chromatogr.*, 91 (1974) 313.
13 Chromatography Group of the Institute of Chemistry, Academia Sinica, *Fenxi Huaxue*, in press.
14 W. T. Wang *et al.*, *Fenxi Huaxue*, in press.
15 Research Paper, Academy of Chemical Engineering Research, Peking, March 1977.
16 H. F. Liu, *Fenxi Huaxue*, in press.

17 Chromatography Group of the Institute of Chemistry, Academia Sinica, *Huaxue Yenjiu*, 2 (1977) 12.
18 S. Setsuya and T. Hidekuni, *Hitachi Sci. Instrum. News*, 17, No. 4/5 (1974).
19 Z. M. Yan and C. Y. Chang, *Measurement and Calculation of Surface Area and Pore Size Distribution of Powder*, Institute of Chemistry, Academia Sinica, Peking, 1977.
20 N. Takai and T. Yamable, *Seisan Kenkyu*, 26 (1974) 278.
21 M. E. van Kreveld and N. van den Hoed, *J. Chromatogr.*, 83 (1973) 111.